Carbon Dioxide−Induced Swelling of Poly(dimethylsiloxane)

ARTICLE *in* MACROMOLECULES · DECEMBER 1999

Impact Factor: 5.8 · DOI: 10.1021/ma9904518

Carbon Dioxide-Induced Swelling of Poly(dimethylsiloxane)

Joseph R. Royer,[†] Joseph M. DeSimone,[†,‡] and Saad A. Khan*[,†]

Department of Chemical Engineering, North Carolina State University, Riddick Hall, Box #7905, Raleigh, North Carolina 27695-7905, and Department of Chemistry, University of North Carolina, Venable and Kenan Laboratories, CB#3290, Chapel Hill, North Carolina 27599

Received March 29, 1999; Revised Manuscript Received October 19, 1999

ABSTRACT: A new experimental device is used to monitor in situ the swelling behavior of poly(dimethylsiloxane) melts in contact with supercritical carbon dioxide. The effects of pressure, temperature, and sample molecular weight on the kinetics and extent of swelling are examined using this experimental technique. The swelling kinetics of all polymer samples exhibit two distinct regimes: an initial region of large swelling in which the diffusion of CO_2 into the polymer follow Fickian behavior and a subsequent region of small volume increase asymptotic to an equilibrium swelling value. Diffusion coefficients of CO_2, obtained from the initial swelling kinetics data, are found to be relatively insensitive to pressure, increase with temperature, and decrease with polymer molecular weight with the latter exhibiting a power-law dependence with an exponent of ~ -2. The extent of swelling increases with both pressure and molecular weight but exhibits different trends with temperature depending on system pressure. For pressures below 15 MPa the extent of swelling decreases monotonically with temperature. However, for pressure above this threshold, a maximum in swelling is observed with temperature increments. The maximum with temperature is thought to be a result of large variations in the physical properties of CO_2 near its critical point. The results of equilibrium swelling have been modeled using the Sanchez−Lacombe equation of state and found to be in good agreement with the thermodynamic theory.

Introduction

Over the past decade, the use of supercritical fluids (SFCs), especially carbon dioxide, to selectively control and manipulate the physical properties of polymer melts during synthesis and processing has become an area of considerable importance in polymer science.[1] The unique ability to *tune* the physical properties of SCFs, by changing pressure and temperature, allows for greater control of a polymer's physical properties compared to traditional polymeric additives, which are often difficult to precisely control and separate. Several research groups have already demonstrated the utility of pressure-tuning supercritical carbon dioxide ($scCO_2$) in synthesis,[2−5] foaming,[6,7] and rheological modification.[8−12] All of the specific processes tend to exploit the swelling and plasticization of the polymer, which results from the inclusion of a large amount of the SCF into a polymer matrix under pressure.

It is well established that when a polymer comes into contact with a low-molecular weight material, sorption of the low-molecular weight species by the polymer often occurs. When the absorption is accompanied by an increase in the linear dimension of the polymer, it is commonly referred to as swelling. The swelling of polymers involves either mutual dissolution of two completely miscible substances (solvent and polymer) or solution of the low-molecular-weight component into the polymer. Both situations result in increased mobility of the polymer phase, which has been shown to modify reaction kinetics, improve diffusion of small molecules,[13] and reduce polymer glass transition temperature (T_g).[14−16]

While CO_2-induced plasticization and T_g depression have been extensively studied for many systems,[14−16] the degree to which $scCO_2$ actually swells a given polymer matrix has been largely ignored. Wissinger and Paulaitis[16,17] have published the most extensive results on the swelling and sorption of polymer−CO_2 mixtures; however, their studies focused on glassy polymers such as polycarbonate, poly(methyl methacrylate), and polystyrene, well below their T_g's. The swelling experiments were therefore conducted on polymers in the *solid* state and in a limited pressure range between 0 and 10 MPa. Our experiments encompass an extended pressure range of 0−30 MPa and, more importantly, focus on melt phase polymers, which are considerably more difficult to undertake. Other studies in this area have investigated swelling of *cross-linked* derivatives of melt phase polymers such as PDMS,[18,19] the results of which cannot be directly carried over for the melt phase. Garg et al.[20] are the only group that reports on an estimation of the swelling of PDMS. They modeled solubility data using the Sanchez−Lacombe equation of state and then used that to predict the swelling behavior of PDMS; however, no direct measurement of the equilibrium swelling was reported.

In this paper, we present a novel technique for measuring the swelling and solubility of $scCO_2$ in polymer melts. We examine three different molecular weight samples of poly(dimethylsiloxane) (PDMS) and discuss swelling and diffusion of CO_2 in relation to system temperature and pressure, CO_2 density, and the molecular weight of PDMS. The swelling data are also modeled using the Sanchez−Lacombe equation of state. We believe, to the best of our knowledge, that this study represents one of the first investigations of the swelling (both equilibrium and kinetics) of an un-cross-linked polymer melt under high-pressure conditions.

Experimental Materials and Methods

Materials. Three different PDMS samples were used as received for our study. Two of these samples, VISCASIL 12-M

[†] North Carolina State University.
[‡] University of North Carolina.
* To whom correspondence should be addressed: Ph 919-515-4519; Fax 919-515-3465; e-mail khan@eos.ncsu.edu.

10.1021/ma9904518 CCC: $18.00
Published on Web 11/25/1999

Table 1. GPC Data of the Three Poly(dimethylsiloxane) Samples

sample	M_n ($\times 10^{-4}$ g/mol)	M_w ($\times 10^{-4}$ g/mol)	PDI
V-12M	4.4	9.5	2.2
V-100M	7.0	16.0	2.3
PS049.5	12.1	28.4	2.3

and VISCASIL100-M, were obtained from General Electric (Waterford, NY), while the third, PS049.5, was obtained from United Chemical Technologies (Bristol, PA). All samples were clear, trimethylsiloxy-terminated poly(dimethylsiloxane) with no suspended particulate matter. The standard kinematic viscosity of the VISCASIL 12-M, VISCASIL-100M, and PS049.5 were 12 500, 10^5, and 10^6 cSt, respectively. Gel permeation chromatography performed on these samples, using toluene as a solvent, revealed all samples to have a polydispersity index of about 2.2 and VISCASIL 12-M, VISCASIL100-M, and PS049.5 to have molecular weights of 95, 160, and 284 kg/mol, respectively. Further details of the samples are provided in Table 1. Liquid carbon dioxide (bone dry grade 2.8) (purity >99.8%) was obtained from National Welders and used as received.

Swelling Apparatus. Measurements of the swelling kinetics and CO_2 diffusion were performed in a specially designed high-pressure view cell, constructed of 316 stainless steel. A schematic representation of the cell, which was designed to constrain the diffusion of CO_2 and the swelling of the polymer to one dimension, is shown in Figure 1. The inside of the cell is rectangular in shape, with dimensions of 0.635 cm (width), 1.587 cm (depth), and 1.587 cm (height) and an approximate volume of 1.7 cm^3. The corners of the interior of the cell were machined to ensure minimal curvature and to maintain the desired rectangular shape. The window housing of the cell consisted of a steel plug in series with a brass O-ring, a 1.25 cm thick sapphire window (2.54 cm o.d.), and a 0.005 cm thick Teflon gasket. The Teflon gasket was hand cut to ensure that the volume between the sapphire window and the steel cell was minimal. While the volume between the sapphire window and the steel cell is not rectangular in shape due to the gasket, it consists of less than 1% of the total sample volume and therefore adds minimal error to the measurement.

Temperature control of the cell was maintained using an autotune temperature control unit (Omega CN77353-A2) in conjunction with a type-K thermocouple. The entire cell was enclosed in a laboratory oven with ventilation to create uniform heating in the cell. The pressure within the cell was monitored using an output pressure transducer (Omega PX302-10KGV) accurate to 0.25% full scale (~0.1 MPa). The cell was also equipped with a 50 MPa rupture disk. High-pressure CO_2 was introduced to the cell using a syringe pump (Isco 260D).

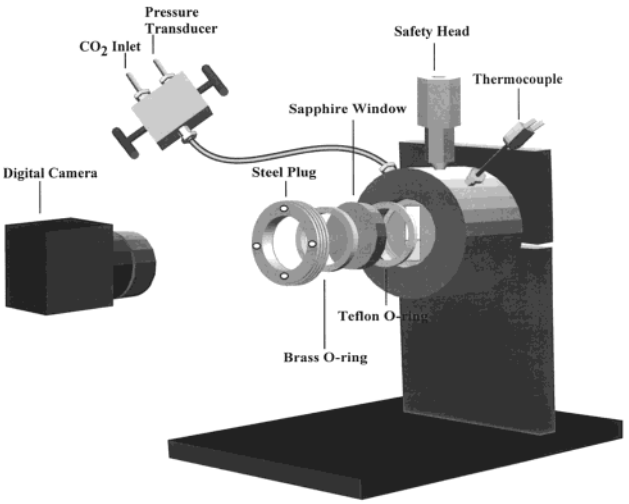

Figure 1. Schematic diagram of the high-pressure swelling apparatus designed for detecting a one-dimensional volume expansion of a polymer melt.

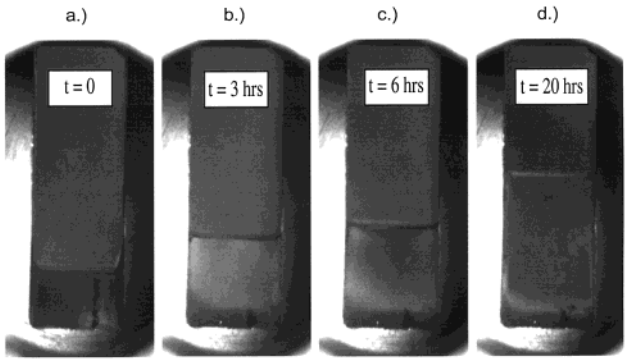

Figure 2. Optical monitoring of the swelling behavior of the PDMS sample at 20.7 MPa and 70 °C. Images are shown for various times after exposure to CO_2: (a) Initial time $t = 0$, (b) 0.3 h, (c) 3 h, and (d) 15 h.

A digital camera (Pulnix TM-7CN) outfitted with a 50 mm lens (Nikon f/1.4D) was used to capture stop motion images of the swelling polymer/CO_2 system in real time. The information from the digital camera was recorded on a personal computer utilizing an image capture board (Scion Corp LG3) and NIH imaging software.

Swelling Procedure. At the beginning of each experimental run, the cell was thoroughly cleaned with THF and acetone, dried with compressed air, and purged several times with high-pressure CO_2. Approximately 0.2 g of the PDMS fluid was injected into the cell through the 1/16 in. connection drilled into the top of the rectangular chamber. The cell was then sealed and evacuated using a vacuum pump to remove any gas that could previously have been dissolved in the polymer. Once the system reached thermal equilibrium (at the set temperature), high-pressure CO_2 was injected into the cell using the same 1/16 in. connection as was previously used to inject the polymer. The digital camera in conjunction with the NIH imaging software was then used to capture a series of images at constant time intervals. The typical time lag between injection of the CO_2 and the first image was approximately 5 s. The images were collected until no further swelling was detected (typically ~24 h) to ensure that the equilibrium was attained. Figure 2 shows a set of images during the swelling of PS049.5 sample (M_w = 284 kg/mol) at 70 °C and 20.7 MPa. In this case, equilibrium was reached within 20 h with the sample doubling its volume in that time period. To obtain quantitative information from the images, the imaging software was used to correlate the number of pixels to the height of the PDMS for each individual picture. From this information, and the calibration of the pixels using the dimensions of the cell, kinetic information on polymer swelling could be determined.

Results and Discussion

Swelling Kinetics. The kinetics of swelling of a typical PDMS sample in CO_2 is illustrated in Figure 3. In this figure, the volume of the 9.5×10^4 g/mol PDMS sample under 20.7 MPa and 50 °C is shown as a function of time. There are several notable features to the curve. The initial slope of the curve is directly related to the Fickian diffusion coefficient. In fact, the first 60% of the swelling curve data plotted as a function of the square root of time reveals a linear relationship (see inset). However, the sharp curvature near equilibrium generally associated with Fickian behavior[21] is not present in Figure 3. Instead, a slower approach to equilibrium, in the neighborhood of maximum swelling, is apparent. The most probable explanation for this phenomenon is that the large degree of swelling in the system actually distorts this region of the curve. Mazich et al. have investigated the kinetics of solvent swelling in elastomeric systems using a mathematical model

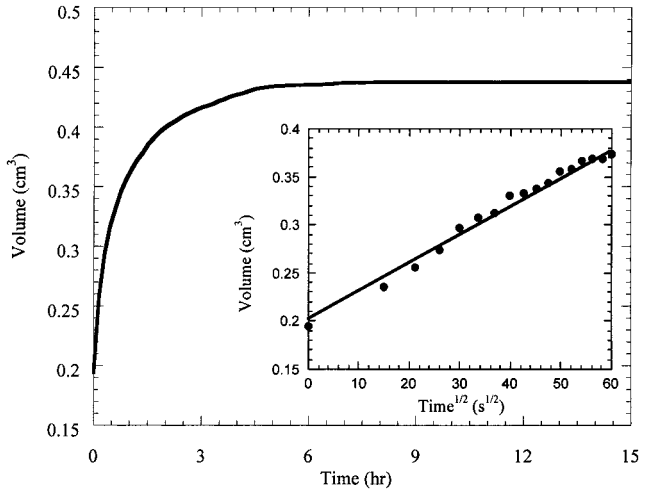

Figure 3. Swelling kinetics for the 95 000 g/mol PDMS sample exposed to CO_2 at 20.7 MPa and 50 °C. Inset figure demonstrates the linear relationship obtained when the initial 60% of the kinetic data are shown as a function of $t^{1/2}$.

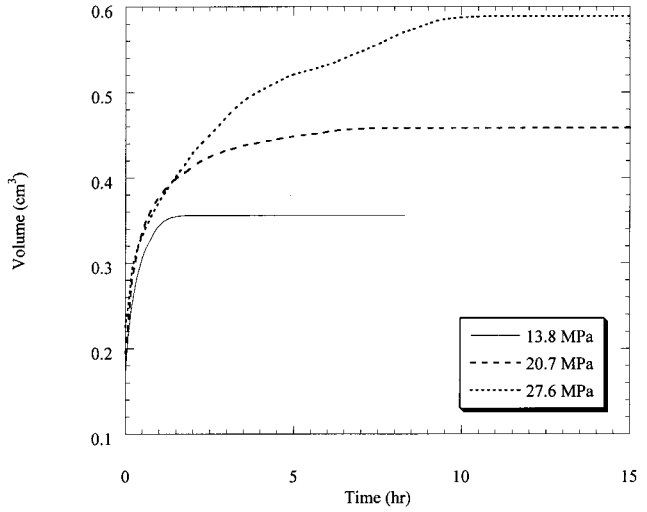

Figure 4. Swelling kinetics for the 160 000 g/mol PDMS sample exposed to CO_2 at 50 °C and various pressures.

based on Fickian principles that uses a transformation of variables so as to directly map the swelling in an imaginary coordinate system.[22−24] They were able to elegantly show that these features of polymer swelling that are usually described as "non-Fickian" can in fact be found a consequence of Fick's law when the swelling of the polymer chains as solvent diffuses in is properly taken into account.

The effects of system pressure on the kinetics of swelling are examined in Figure 4 for the 9.5×10^4 g/mol PDMS at 50 °C. In this figure, which shows data for three different pressures (13.8, 20.7, and 27.6 MPa), significant differences are observed in the actual equilibrium swelling value and the time required to reach equilibrium. We find that while the swelling of the system increases with pressure, the time required to reach equilibrium also increases. In the 13.8 MPa experiment, the time to reach equilibrium is approximately 2 h as compared to 7 and 10 h for the 20.7 and 27.8 MPa systems, respectively. The degree of swelling also increases by almost a factor of 2 as pressure is increased from 13.8 to 27.8 MPa.

Figure 5 shows the effect of temperature (30, 50, and 70 °C) on the kinetic rate of swelling at a constant

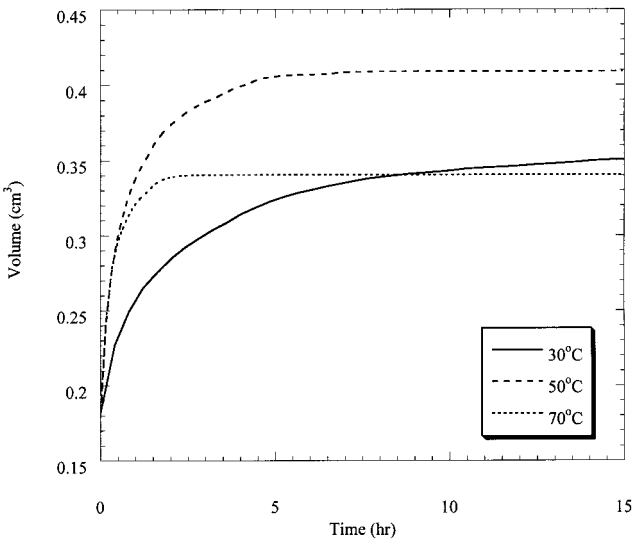

Figure 5. Swelling behavior as a function of time for the 95 000 g/mol PDMS sample exposed to CO_2 at 20.7 MPa and various temperatures.

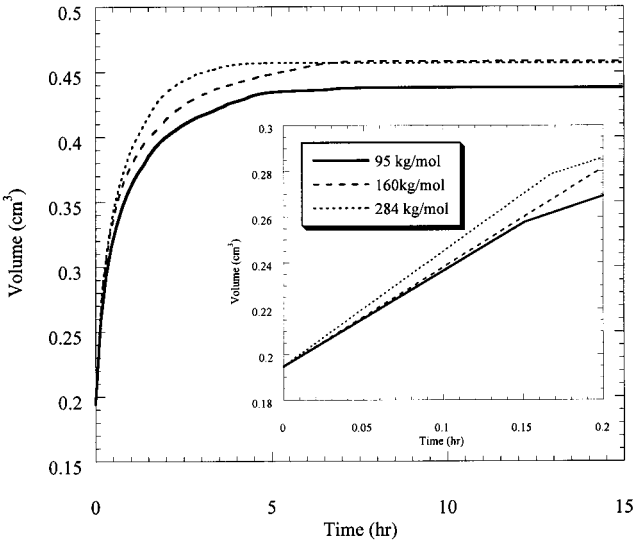

Figure 6. Swelling kinetics for PDMS exposed to CO_2 at 20.7 MPa and 50 °C for various molecular weights. Inset figure displays a close-up view of the initial portion of the kinetic curves to demonstrate more clearly the effect of molecular weight.

pressure of 20.7 MPa. For the 9.5×10^4 g/mol PDMS sample shown in this figure, three distinct features are apparent from the data. First, the initial slopes of the swelling curves at the three temperatures are different. This phenomenon is directly dependent on the diffusion coefficient of the system, as previously mentioned, and suggests that the diffusion coefficient of the system increases with temperature. Second, the time required to reach equilibrium decreases with temperature from 13 h at 30 °C to 7 h at 50 °C to 2 h at 70 °C. This again suggests that the diffusion coefficient of the system is increasing with temperature. Finally, the actual equilibrium value of the swelling increases as temperatures is increased from 30 to 50 °C but drops to its lowest value at 70 °C. This indicates that polymer swelling undergoes a maximum as a function of temperature.

The effect of molecular weight on the polymer swelling rate is illustrated in Figure 6 at 20.7 MPa and 50 °C. Molecular weight seems to have a small effect on the equilibrium value of swelling and the shape of the

kinetic curve. One reason for such a low sensitivity of swelling to molecular weight could be the range of molecular weights investigated. The three molecular weights chosen for this study are all well above the critical molecular weight for entanglements of PDMS, which is approximately 2.8×10^4 g/mol.[25] When experiments are done on samples well below and near the critical entanglement molecular weight, the effect of the molecular weight on swelling could be different. In fact, at a molecular weight of approximately 1.5×10^4 g/mol, we have found the polymer to become soluble at a pressure of 20.7 MPa at 50 °C. The molecular weight does however have an effect on the initial slopes of the curves (see inset), with the initial slope of the kinetic curves decreasing with higher molecular weights. This phenomenon is discussed further in the following section as it relates directly to the molecular weight dependence of CO_2 diffusion into the melt.

Diffusion Coefficients of CO_2 into PDMS. The first region of the swelling kinetics curves examined in the previous section can be directly related to the diffusion coefficient of CO_2 into PDMS using Fick's law:

$$\frac{\partial c}{\partial t} = \frac{\partial^2 (Dc)}{\partial z^2} \tag{1}$$

Here, c is the penetrant concentration, t is time, and D is the diffusion coefficient. To solve the above equation, we assume the polymer to be a semiinfinite medium in the limit of short times. This is a reasonable assumption as the polymer contains no CO_2 initially and allows for the modification of the boundary conditions to establish what amounts to an infinite driving force. This assumption has been proven to be valid for up to approximately 60% of the equilibrium swelling for systems that demonstrate Fickian behavior.[21]

A similarity transform can then be employed to solve the above differential equation with the boundary conditions specific to this problem. This method gives the following expression for the mass of penetrant (M_t) taken up into the polymer sample as a function of time:

$$M_t = 2\rho_{CO_2} c_\infty \left(\frac{Dt}{\pi}\right)^{1/2} S_A \tag{2}$$

Here, S_A is the surface area and c_∞ is the CO_2 concentration at equilibrium.

Defining the degree of swelling, α, in the following manner

$$\frac{\alpha}{\alpha_\infty} \equiv \frac{V_t - V_0}{V_\infty - V_0} = \frac{M_t}{M_\infty} \tag{3}$$

allows the mass uptake of the system to be directly related to the degree of swelling. Equation 3 is valid only if the volume change of mixing is zero and mass uptake and volume expansion are directly equivalent. If the volume change upon mixing of the two components is significant, the equation must be modified to account for the change in difference in mass addition to volume expansion. Expressing the total mass uptake as $M_\infty = \rho_{CO_2} l_\infty S_A c_\infty$ (l_∞ is the height at equilibrium), substituting it into eq 3, and combining with eq 2, an equation that relates swelling to the diffusion coefficient can be obtained.[26−28]

$$\frac{\alpha}{\alpha_\infty} = \frac{2}{l_\infty}\left(\frac{Dt}{\pi}\right)^{1/2} \tag{4}$$

This expression can be fit to the initial portion of the swelling kinetics curve to obtain a diffusion coefficient of CO_2 in PDMS. For this analysis to be valid, the assumptions made in eq 3 must be satisfied, specifically that the volume change on mixing is negligible. In our system, once the CO_2 was charged to the cell, the entire system was sealed. During the swelling process, minimal pressure change on the order of the error in the pressure transducer (<0.2 MPa) was detected, and therefore we feel justified in claming that the volume change with mixing is negligible. Such an approach has been used by Garg et al. to model the solubility behavior of PDMS with CO_2 for a polymer of molecular weight 30.8×10^4 g/mol.[20] They argued that when the CO_2 is subcritical, the volume changes upon dissolution of the gas into the polymer melt are highly nonideal but tend toward ideal mixing at supercritical conditions. Almost all of our experiments were conducted under supercritical conditions when near ideal-mixing conditions prevail.

Figure 7 presents the diffusion coefficients obtained for the 9.5×10^4 g/mol PDMS sample as a function pressure for three different temperatures. We find the diffusion coefficient of CO_2 increases as the temperature of the system increases. This result is expected because the short scale molecular motions of the polymer should increase as the temperature increases, allowing the CO_2 to penetrate the polymer matrix more easily. The effect of pressure on the diffusion coefficient appears to be much less pronounced. In general, as the pressure increases, the diffusion coefficient decrease slightly. This is because the polymer will be compacted/compressed more with increased pressure. This however is not expected to be significant because under the pressure conditions of our experiments pure PVT data show density changes in the PDMS melt to be less than 5%.[29]

The effect of molecular weight on the diffusion coefficient is presented in Figure 8. This figure demonstrates that an increase in the molecular weight of the polymer tends to decrease the diffusion coefficient of the CO_2 into the polymer matrix. This effect possibly occurs because of the increased viscosity and number of

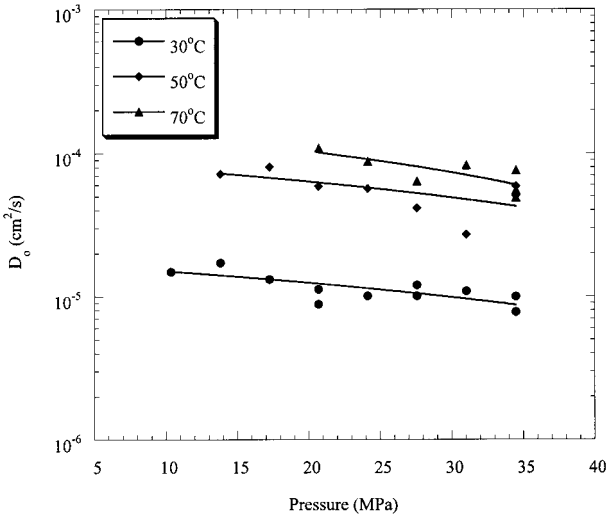

Figure 7. Calculated diffusion coefficients for the 95 kg/mol PDMS sample exposed to CO_2 at various pressures and temperatures.

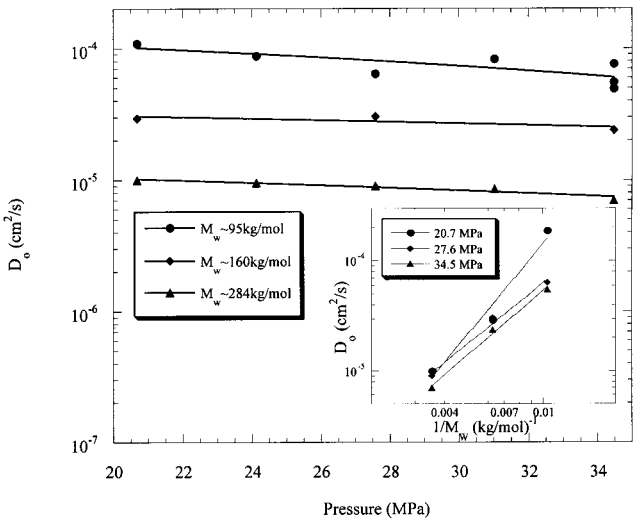

Figure 8. Calculated diffusion coefficients for three PDMS samples exposed to CO_2 at various pressures and 70 °C. The inset shows the molecular weight dependence of the calculated diffusion coefficients at various pressures.

entanglements of the polymer melt at high molecular weights. As the CO_2 diffuses into the polymer, the matrix must expand to accommodate the absorbed CO_2. This causes the entanglements to stretch. Because of the higher viscosity, the ability of the polymer chains to rearrange and accommodate the CO_2 molecules decreases with higher molecular weights. In the inset of Figure 8, the diffusion coefficients at constant pressure are plotted versus $1/M_w$ at 70 °C. The effect of molecular weight appears to show a power law behavior. The dependence of diffusion coefficient on inverse molecular weight appears to have a power law exponent of 2.0 ± 0.5. Interestingly, reptation theory[30,31] predicts that the self-diffusion coefficient should scale as M_w^{-2}. This suggests that the rate of diffusion is largely controlled by the reptation and self-diffusion of the polymer melt itself.

Equilibrium Swelling. The equilibrium swelling can be examined further in terms of the equilibrium swelling ratio defined as

$$\text{equilibrium swelling ratio} = \xi = \frac{V_\infty}{V_0} \qquad (5)$$

where V_∞ is the volume of the polymer sample at equilibrium and V_0 is the initial volume of the polymer. It is important to realize that the temperature, pressure, and CO_2 density all contribute to the value of the equilibrium swelling ratio, and decoupling their effects is difficult. In Figure 9a, the equilibrium swelling ratio is displayed as a function of CO_2 density for the 9.5×10^4 g/mol sample at three different temperatures. Since changing either temperature or pressure can vary CO_2 density, this figure represents the case where density has been varied by changing system pressure. Figure 9a reveals that the extent of swelling increases with increasing CO_2 density and therefore with increasing system pressure at a constant temperature. (*Lines are drawn to illustrate trends and not theoretical predictions.*) We observe a similar trend of increased swelling with increasing density for all measured temperatures, with the extent of swelling curves shifting to higher values at higher temperatures, at a constant density. It is, however, important to point out that the same CO_2 density does not correspond to the same swelling at different temperatures. This is because increasing the temperature of the system shifts the isotherms toward the direction of lower CO_2 density. Therefore, to maintain a constant CO_2 swelling the system pressure must be increased, and that would tend to increase the equilibrium swelling. This problem exemplifies the difficulty in decoupling the effects of pressure, temperature, and CO_2 density. While CO_2 density is not specifically an independent parameter, it does undergo large changes around the critical point and vary nonlinearly with temperature and pressure. CO_2 density has been used as a measure of solvent quality, but it is important to also consider the effects of temperature and pressure on density.

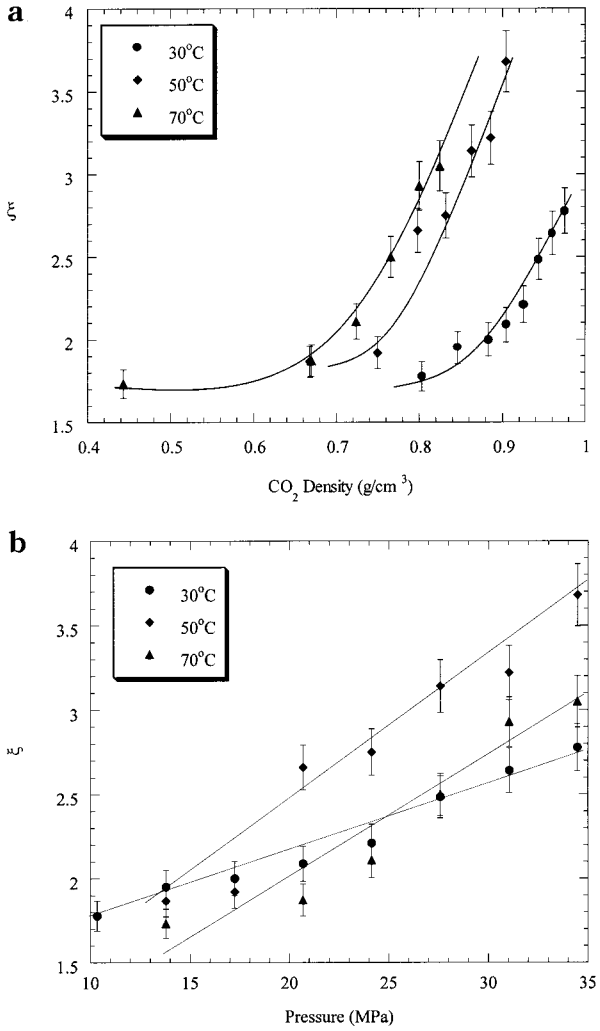

Figure 9. Isothermal data for the equilibrium swelling ratio, ξ, for the 95 000 g/mol PDMS sample exposed to CO_2 at various pressures (a) shows data as a function of CO_2 density whereas (b) reveals the data as a function of system pressure. Lines are drawn to illustrate trends and not theoretical predictions.

The same data for the 9.5×10^4 g/mol sample are plotted as a function of system pressure in Figure 9b. It is clearly shown that the equilibrium swelling ratio increases monotonically with increasing pressure. However, it is quite apparent that the effect of system pressure is different at different temperatures, a facet that is not observed from Figure 9a. Specifically, the data at 30 °C have a slope that is much flatter than that of the other two temperatures (50 and 70 °C). It is interesting to note that 30 °C is just slightly (1 °C) below

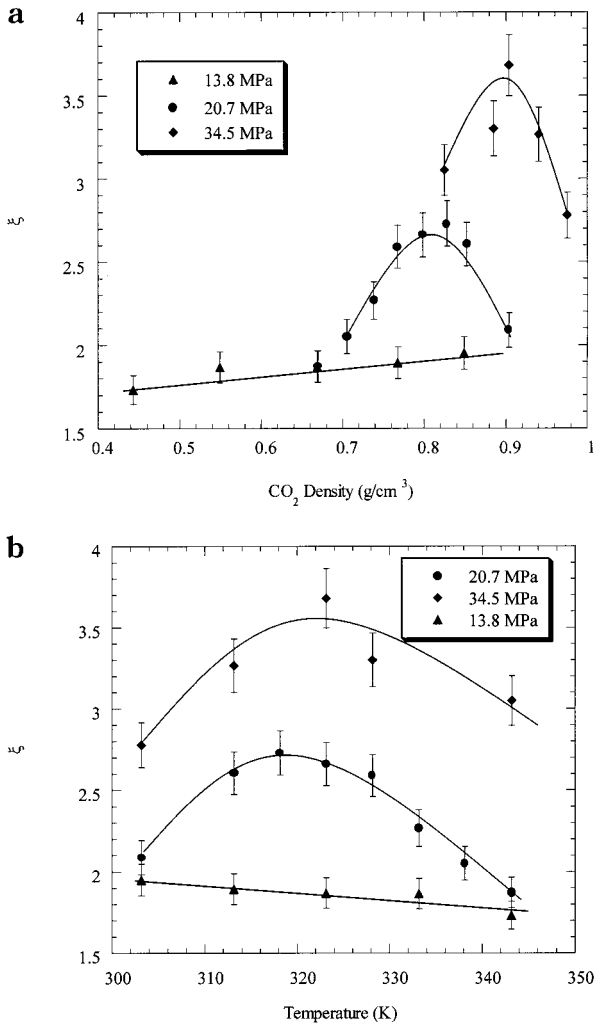

Figure 10. Isobaric data for the equilibrium swelling ratio, ξ, for two different molecular weight samples exposed to CO_2 at various temperatures and pressures. Data are shown as both as a function of CO_2 density (a) and as a function of system pressure (b). Lines are drawn to illustrate trends and not theoretical predictions.

the critical temperature and that the other two data sets are systems where the CO_2 is well within the supercritical region. By comparing the data points at constant pressure as a function of temperature in Figure 9b, it is clear that at approximately 15 MPa a maximum in swelling ratio will occur. This can be seen by noting that the data for both the 30 and 70 °C curves are lower than the 50 °C curve, indicating a maximum between 30 and 70 °C. Below this crossover pressure, no maximum should be apparent.

To test this hypothesis, we have plotted the effects of temperature on the equilibrium swelling ratio, independent of the system pressure. In Figure 10a, the equilibrium swelling ratio is plotted against CO_2 density just as in Figure 9a, except here decreasing temperature increases the CO_2 density. The experimental results for the 9.5×10^4 g/mol PDMS sample at two different pressures, 20.7 (circles) and 34.5 MPa (diamonds), clearly demonstrate that the equilibrium swelling exhibits a maximum with increased CO_2 density (or decreased temperature) at constant pressure. (*Once again lines are drawn to illustrate trends and not theoretical predictions.*) It is important to note that the maximum does not correspond to a specific density of

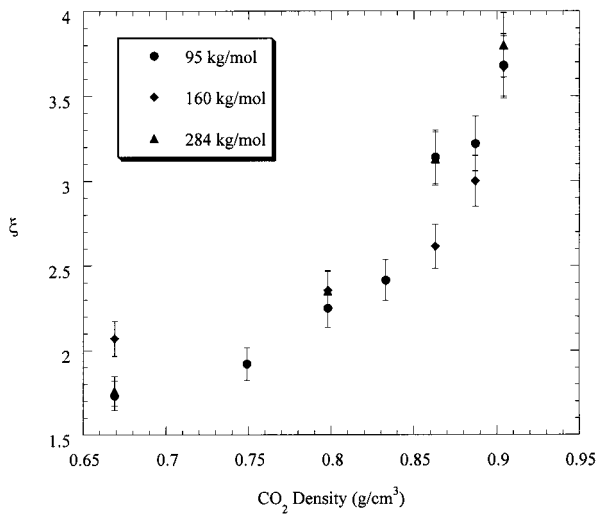

Figure 11. Isothermal data for the equilibrium swelling ratio, ξ, for three different molecular weight samples exposed to CO_2 at various pressures and 50 °C as a function of CO_2 density.

the CO_2 mixture and that the maximum equilibrium swelling ratio increases with pressure.

Figure 10b shows the data for the same PDMS sample plotted as a function of temperature. We find the equilibrium maximum to occur at about the same temperature (48 ± 2 °C) independent of pressure. Experiments conducted at different molecular weights (*data not shown*) show the same trend with negligible effect of molecular weight. Figure 10a also shows the effect of CO_2 density on the same PDMS at a subcrossover pressure of 13.8 MPa. We find no maximum in the extent of swelling, but rather a monotonic increase with CO_2 density. The same data plotted as a function of temperature show a monotonic decrease with increasing temperature. These two data sets are consistent as increases in the temperature corresponds to decreases in density. The absence of a maximum in these figures plots corroborates with Figure 9b; however, the only explanation that we can offer is that, in subcritical conditions (below 30 °C) and near the critical temperature, the mechanism for CO_2-induced swelling of the PDMS melt maybe slightly different than that of supercritical conditions, causing this maximum to occur at pressures greater than 15 MPa.

Figure 11 displays the equilibrium swelling ratio for all three molecular weight samples at 50 °C as a function of CO_2 density. It is evident from this figure that no dependence of the equilibrium swelling ratio on polymer molecular weight can be determined within the error of the experimental apparatus (~3−4%). Once again it is important to point out that these samples all have molecular weights much greater than the entanglement molecular weight, and the inability to distinguish between molecular weights may be limited to this regime.

Modeling of Equilibrium Swelling. The solubility of high-pressure gases in polymer melts has traditionally been modeled using the Sanchez−Lacombe equation of state (S−L EOS).[8,20,32] With proper manipulation of the calculated solubilities it is possible to use the S−L EOS to predict the equilibrium swelling behavior of the supercritical fluid/polymer systems. The S−L EOS, which is a lattice fluid equation of state, is derived from

Table 2. Sanchez−Lacombe Pure Component Characteristic Parameters

substance	ρ^*(g/cm^3)	P^* (MPa)	T^* (K)	ref
PDMS	1.104	302.0	476.0	33
CO_2	1.426	464.2	328.1	20
	1.430	458.0	330.4	20
	1.510	574.5	305.0	32

Flory−Huggins theory[33−35] and is given by

$$\tilde{\rho}^2 + \tilde{P} + \tilde{T}\left[\ln(1-\tilde{\rho}) + \left(1 - \frac{1}{r}\right)\tilde{\rho}\right] = 0 \tag{6}$$

Here, r represents the number of lattice sites occupied by a molecule, and $\tilde{\rho}$, $\tilde{P}$, and $\tilde{T}$ are the reduced density, pressure, and temperature, respectively. The reduced parameters are defined by the ratio of the system variables to the characteristic properties as follows:

$$\tilde{\rho} = \frac{\rho}{\rho^*} \quad \rho^* = \frac{M}{rv^*} \quad \tilde{v} = \frac{1}{\tilde{\rho}}$$
$$\tilde{P} = \frac{P}{P^*} \quad P^* = \frac{\epsilon^*}{v^*}$$
$$\tilde{T} = \frac{T}{T^*} \quad T^* = \frac{\epsilon^*}{R} \tag{7}$$

where ρ^*, P^*, T^*, and v^* are the characteristic density, pressure, temperature, and volume, respectively, ϵ^* is the characteristic interaction energy per mer, and R is the gas constant. The characteristic parameters used for the reduced properties are obtained by fitting pure-component PVT data using a least-squares analysis. Sanchez and Lacombe[33] have suggested a set of values for PDMS, and several sets are available for CO_2.[8,20] A list of the pure-component characteristic properties for this experimental system is given in Table 2.

To apply the equation of state to a mixture of two fluids, the mixing rules for the characteristic parameters must be defined. There are several sets of mixing rules commonly used in the literature.[8,20,32−35] Because the model has three independent characteristic parameters, three mixing rules are required. Once the three mixing properties are defined, the remainder of the mixture properties can be found by evaluating the relations in eq 6 for the mixture. We have chosen to use the so-called van der Waals-1 rules[36] that assume random mixing of the components.

The first mixing rule is applied to find the closed-packed molar volume of a mer of the mixture v^*_{mix}

$$v^*_{mix} = \sum_{i=1}\sum_{j=1}\phi_i\phi_j v^*_{ij} \tag{8}$$

with

$$v^*_{ij} = \frac{v^*_{ii} + v^*_{jj}}{2}(1 - n_{ij}) \tag{9}$$

where η_{ij} is the volume correction factor, correcting for deviations from the arithmetic means and where the subscripts refer to the two components of the system. ϕ_i is the volume fraction of component i in the mixture defined as

$$\phi_i = \frac{\dfrac{m_i}{\rho^*_i v^*_i}}{\displaystyle\sum_{j=1}\frac{m_j}{\rho^*_j v^*_j}} \tag{10}$$

where m_i is defined as the mass fraction of component i. The second mixture rule defines the characteristic interaction energy for the mixture ϵ^*_{mix}

$$\epsilon^*_{mix} = \frac{1}{v^*_{mix}}\sum_{i=1}\sum_{j=1}\phi_i\phi_j\epsilon^*_{ij}v^*_{ij} \tag{11}$$

with

$$\epsilon^*_{ij} = \sqrt{\epsilon^*_{ii}\epsilon^*_{jj}}(1 - k_{ij}) \tag{12}$$

Here k_{ij} is a mixture parameter that accounts for specific binary interactions between components i and j similar to the Peng−Robinson equation of state.[36] The final mixing rule is for r_{mix}, the number of sites occupied by a molecule of the mixture:

$$\frac{1}{r_{mix}} = \sum_{j=1}\frac{\phi_j}{r_j} \tag{13}$$

Using these mixing rules the equations of state (5) can be evaluated at any given mass fraction m_i. To obtain a model of the equilibrium mixture, it is necessary to impose thermodynamic constraints on the system as follows:

$$T^{\mathrm{I}} = T^{\mathrm{II}}$$
$$P^{\mathrm{I}} = P^{\mathrm{II}}$$
$$\mu_i^{\mathrm{I}} = \mu_i^{\mathrm{II}} \quad \text{(for all } i\text{)} \tag{14}$$

where μ is the chemical potential and the superscripts I and II refer to the two phases in equilibrium. The chemical potential for component i in a mixture can be evaluated using the following equation derived from the S−L EOS.

$$\mu_i = RT\left[\ln\phi_i + \left(1 - \frac{r_i}{r}\right)\right] + r_i\left\{-\tilde{\rho}\left[\frac{2}{v^*}\left(\sum_{j=1}\phi_j v^*_{ij}\epsilon^*_{ij} - \epsilon^*\sum_{j=1}\phi_i v^*_{ij}\right) + \epsilon^*\right]\right\} + r_i\left\{RT\tilde{v}\left[(1-\tilde{\rho})\ln(1-\tilde{\rho}) + \frac{\tilde{\rho}}{r_i}\ln(\tilde{\rho})\right] + P\tilde{v}\left(2\sum_{j=1}\phi_i v^*_{ij} - v^*\right)\right\} \tag{15}$$

where unsubscripted variables refer to mixture or system properties. By substituting pure component properties for those of the mixture and setting the closed packed volume fraction of component i to 1, the expression for the pure component chemical potential can be attained. Forcing the pure CO_2 chemical potential to equal to the chemical potential of CO_2 in the mixture defines the equilibrium state. A Fortran program of the from proposed by McHugh[36] is used to solve this set of equations (5−14) to obtain values for the solubility of

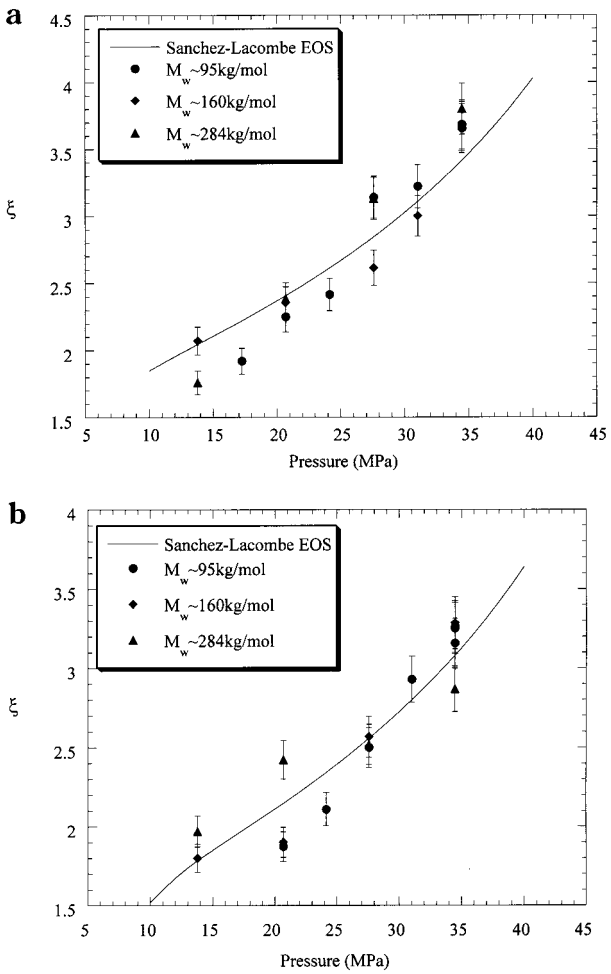

Figure 12. Theoretical prediction of the isothermal equilibrium swelling ratio, ξ, using the Sanchez−Lacombe equation of state for three different molecular weight samples exposed to CO_2 at various pressures and (a) 50 °C and (b) 70 °C.

CO_2 in the polymer melts as a function of temperature and pressure.

To compare the S−L EOS prediction directly to the data collected in our experiments, it is necessary to derive an expression that predicts the swelling of the polymer-rich phase at equilibrium. Starting with a known initial density of the polymer phase, ρ_p, and the density of the polymer-rich phase obtained from the equation of state model, ρ_{mix}, in conjunction with the calculated equilibrium mass fraction of m_p, the equilibrium swelling ratio is defined as follows:

$$\frac{V_\infty}{V_0} = \frac{\rho_p(1 - m_p)}{m_p \rho_{mix}} \tag{16}$$

This equation will now allow us to predict the equilibrium swelling ratio of the PDMS−CO_2 system using pure component PVT data and then adjusting the binary interaction parameters. Using eq 16, predictions of the swelling at 50 and 70 °C are presented in Figure 12. The prediction is not done at 30 °C because in the neighborhood of the critical point the S−L EOS prediction of the pure CO_2 PVT properties is extremely poor and therefore would provide minimal insight.

Figure 12a displays the experimental and predicted values of the equilibrium swelling ratio for all three molecular weight samples as a function of system pressure at 50 °C. Figure 12b also shows data for all three molecular weight samples as a function of system pressure at 70 °C. The two adjustable binary interaction parameters κ_{ij} and η_{ij} have been fit to the experimental data using a least-squares analysis of the governing equations. The values of these two parameters for the two different temperatures are found in Table 3.

Table 3. Binary Interaction Parameters Obtained by Fitting the Experimental Swelling Data to the Sanchez−Lacombe Equation of State

temperature (°C)	η_{ij}	k_{ij}
50	−0.012	0.15
70	−0.0275	0.17

The close agreement of the theoretical prediction to the measured physical properties of the CO_2-swollen polymer melt demonstrates the ability of the Sanchez−Lacombe equation of state to effectively model the swelling behavior of high-pressure CO_2 in an amorphous polymer melt. It is important to note that the curve fits to the experimental data between each of the three molecular weights are indistinguishable. Therefore, we are only presenting one curve as a representative fit to the data at all three molecular weights. It is possible that at lower molecular weights near the entanglement molecular weight the swelling and solubility of CO_2 in the melt, and the Sanchez−Lacombe EOS theory will show a much greater dependence on molecular weight.

Conclusions

A novel experimental setup was designed to investigate in situ the swelling behavior of a polymer melt in contact with a high-pressure fluid. This approach, based on optically monitoring polymer swelling in real time, was used to determine the swelling kinetics, swelling equilibrium, and rates of CO_2 diffusion into poly(dimethylsiloxane) melts of three different molecular weights. We found that the diffusion of CO_2 into PDMS exhibited a Fickian behavior up until two-thirds of the equilibrium swelling value was reached. The CO_2 pressure had a negligible effect on the diffusion coefficient probably due to the insignificant compaction of the polymer with pressure. However, the system temperature directly affected the diffusion coefficient. In addition, the diffusion coefficient exhibited a power-law dependence with molecular weight with an exponent of −2, consistent with reptation theories.

The equilibrium swelling of PDMS were unaffected by molecular weight within the range of molecular weights studied. However, increased pressure enhanced the extent of swelling whereas a maximum was observed with increasing temperature, at pressure above 15 MPa. The latter can possibly be attributed to large changes in the physical properties of CO_2 near the critical point. Below 15 MPa, a monotonic decrease in the equilibrium swelling ratio is observed with increasing temperature. The Sanchez−Lacombe equation of state was found to in good agreement with the experimentally calculated variables and can be used as a predictive tool to obtain physical properties of the CO_2−PDMS system.

Acknowledgment. The authors gratefully acknowledge the support from the Kenan Center for the Utilization of Carbon Dioxide in Manufacturing at North Carolina State University and the University of North Carolina at Chapel Hill for funding this work. They also thank Stephanie Crette (UNC) for assistance with GPC

measurements and Dr. M. Adams (Grenoble, France) and Dr. N. Kenkare (Lucent Technologies) for their insightful comments and suggestions during the preparation of this manuscript.

References and Notes

(1) Shine, A. D. In *Physical Properties of Polymer Handbook*; Mark, J. E., Ed.; AIP Press: New York, 1996; pp 249−256.
(2) DeSimone, J. M.; Guan, Z.; Eisbernd, C. S. *Science* **1992,** *257***,** 945−947.
(3) DeSimone, J. M.; Maury, E. E.; Menceloglu, Y. Z.; McClain, J. B.; Romack, T. J.; Combes, J. R. *Science* **1994,** *265***,** 356−359.
(4) McClain, J. B.; Betts, D. E.; Canelas, D. A.; Samulski, E. T.; DeSimone, J. M.; Londono, J. D.; Cochran, H. D.; Wignall, G. D.; Chillura-Martino, D.; Triolo, R. *Science* **1996,** *274***,** 2049−2052.
(5) Shaffer, K. A.; DeSimone, J. M. *TRIPS* **1995,** *4***,** 146−153.
(6) Goel, S. K.; Beckman, E. J. *AIChE J.* **1995,** *41***,** 357−366.
(7) Goel, S. K.; Beckman, E. J. *Polym. Eng. Sci.* **1994,** *34***,** 1137−1147.
(8) Mertsch, R.; Wolf, B. A. *Macromolecules* **1994,** *27***,** 3289−3294.
(9) Xiong, Y.; Kiran, E. *Polymer* **1995,** *36***,** 4817−4826.
(10) Bae, Y. C.; Gulari, E. *J. Appl. Polym. Sci.* **1997,** *63***,** 459−466.
(11) Gerhardt, L.; Manke, C.; Gulari, E. *J. Polym. Sci., Polym. Phys.* **1997,** *35***,** 523−534.
(12) Gerhardt, L.; Garg, A.; Manke, C.; Gulari, E. *J. Polym. Sci., Polym. Phys.* **1998,** *36***,** 1911−1918.
(13) Kazarian, S. G. *Appl. Spectrosc. Rev.* **1997,** *32***,** 301−348.
(14) Handa, Y. P.; Capowski, S.; O'Neill, M. *Thermochim. Acta* **1993,** *226***,** 177−185.
(15) Chiou, J. S.; Barlow, J. W.; Paul, D. R. *J. Appl. Polym. Sci.* **1985,** *30***,** 2633−2642.
(16) Wissinger, R. G.; Paulaitis, M. E. *Ind. Eng. Chem. Res.* **1991,** *30***,** 842−851.
(17) Wissinger, R. G.; Paulatis, M. E. *J. Polym. Sci., Polym. Phys.* **1987,** *25***,** 2497−2510.
(18) Fleming, G. K.; Koros, W. J. *Macromolecules* **1986,** *19***,** 2285−2291.
(19) Goel, S. K.; Beckman, E. J. *Polymer* **1992,** *33***,** 5032−5039.
(20) Garg, A.; Gulari, E.; Manke, C. W. *Macromolecules* **1994,** *27***,** 5643−5653.
(21) Crank, J. *The Mathematics of Diffusion;* Clarendon Press: Oxford, 1975.
(22) Rossi, G.; Mazich, K. A. *Phys. Rev. A* **1991,** *44***,** R4793−R4796.
(23) Rossi, G.; Mazich, K. *Phys. Rev. E* **1993,** *48***,** 1182−1191.
(24) Mazich, K. A.; Rossi, G.; Smith, C. A. *Macromolecules* **1992,** *25***,** 6929−6933.
(25) Ferry, J. D. *Viscoelastic Properties of Polymers;* Wiley: New York, 1980.
(26) Machin, D.; Rogers, C. E. *Polym. Eng. Sci.* **1970,** *10***,** 300−304.
(27) Mencer, H. J.; Gomzi, Z. *Eur. Polym. J.* **1994,** *30***,** 33−36.
(28) Vasenin, R. M. *Vysokomol. Soedin.* **1964,** *6***,** 624−629.
(29) Zoller, P.; Walsh, D. J. *Standard Pressure−Volume−Temperature Data For Polymers;* Technomic Publishing Co., Inc.: Lancaster, 1996.
(30) DeGennes, P. G.; Leger, L. *Annu. Rev. Phys. Chem.* **1982,** *33***,** 49.
(31) DeGennes, P. G. *Scaling Concepts in Polymer Physics;* Cornell University Press: Ithaca, NY, 1976.
(32) Kiszka, M. B.; Meilchen, M. A.; McHugh, M. A. *J. Appl. Polym. Sci.* **1988,** *36***,** 583−597.
(33) Sanchez, I. C.; Lacombe, R. H. *Macromolecules* **1978,** *11***,** 1145−1156.
(34) Sanchez, I. C.; Lacombe, R. H. *J. Phys. Chem.* **1976,** *80***,** 2352−2362.
(35) Lacombe, R. H.; Sanchez, I. C. *J. Phys. Chem.* **1976,** *80***,** 2568−2580.
(36) McHugh, M.; Krukonis, V. *Supercritical Fluid Extraction: Principles and Practice;* Butterworth-Heinemann: Boston, 1994.

MA9904518